Convective, absolute, and global instabilities of thermocapillary-buoyancy convection in extended layers

Jānis Priede and Gunter Gerbeth
Forschungszentrum Rossendorf, P.O. Box 510119, D-01314 Dresden, Germany
(Received 24 March 1997)

We study the linear stability of thermocapillary-buoyancy convection in an extended liquid layer subject to a longitudinal temperature gradient. It is found that by applying the concepts of convective, absolute, and global instabilities, theory agrees well with experiment. Two different effects due to the lateral walls are considered. First, the stationary disturbance due to the end walls induces a steady wave pattern spreading over the whole layer as the zero-frequency mode becomes convectively unstable. Second, virtual reflections of traveling disturbances by the lateral walls provide the feedback necessary for the onset of a global instability. In the simplest case, a global neutrally stable state is formed by a couple of transverse waves propagating at the same frequency in opposite directions, so that spatial amplification of one wave compensates for the attenuation of the other. However, the most dangerous self-sustained disturbance is set up by a couple of mirror symmetric oblique waves propagating purely spanwise. For purely thermocapillary-driven flow the threshold of self-sustained instability is just slightly higher than that of the convective instability. However, for liquids of large Prandtl number a moderate buoyancy effect may cause a significant stabilization of self-sustained oscillatory instability. [S1063-651X(97)02610-X]

PACS number(s): 47.20.Dr, 47.20.Bp

I. INTRODUCTION

Because surface tension of common liquids decreases with temperature, any nonuniformity of surface temperature drives the liquid at the surface from hot to cold regions. Viscosity and incompressibility of the liquid causes this motion to spread to the underlying bulk liquid. Smith and Davis [1] found that the thermocapillary effect driving such flows can additionally be the cause of a new type of instability called hydrothermal waves, which are predicted to occur as the longitudinal temperature gradient exceeds a certain threshold that depends on the liquid properties and its geometry. The hydrothermal waves are coupled flow and temperature disturbances sustained by both velocity and temperature gradients of the basic flow. Up to now several experiments have been done to verify this prediction [2–5]. However, there are two significant assumptions in the original theory which complicate its straightforward verification. First, a horizontally homogeneous basic flow is assumed. Second, the effect of buoyancy, which is always present in earth experiments, was not taken into account by Smith and Davis [1]. The first assumption is not a crucial problem for the experiment, because an almost homogeneous basic flow can be obtained in a midpart of a sufficiently extended liquid layer [2]. On the other hand, the buoyancy effect can easily be incorporated into the theory [6].

Comparison of predictions of such an advanced theory with results of an adequate experiment [2] reveals a substantial disagreement between both. Although both theory and experiment show that for high-Prandtl-number liquids like silicon oil an oscillatory instability is stabilized with increase of the depth of the layer, the experimentally found threshold of this instability is significantly higher than the predicted one. This disagreement sharply increases with the depth of the layer. Moreover, the experiment shows that for sufficiently deep liquid layers a stationary instability sets in before an oscillatory one, whereas the latter is predicted to be always the most unstable one. So the disagreement between experiment and existing theory is not only quantitative, but also qualitative. Since a properly designed experiment meets the principal assumptions of the theory, the disagreement between both must be due to the latter, which is based on conventional linear stability analysis.

In this paper, we show that linear stability analysis of a homogeneous basic state is able to bring predictions into agreement with experiment when the distinction between the concepts of convective, absolute and global instabilities [7,8] is taken into account. Because up to now this distinction has been ignored for the stability of convective flows in extended liquid layers, we begin by presenting the basic ideas in physically obvious terms. The concepts of absolute and global instability rely essentially on the criterion defining the direction of wave propagation. Our approach in this point differs from the conventional one. We prove that the sign of the real part of group velocity is a correct criterion for a nonconservative medium to determine the direction of propagation of a certain class of most unstable modes. The conventional approach ignores two important effects due to the confining lateral walls always present in real experiments. First, these walls disturb the assumed uniformity of the basic flow. The problem is to evaluate how far this perturbation can spread from the wall. We show that the effect due to the lateral walls can cause a stationary wave pattern spreading through the whole layer when the zero-frequency mode becomes convectively unstable. Second, the lateral walls can reflect convectively unstable disturbances, giving rise to a global instability.

The paper is organized as follows. The theoretical background is discussed in Sec. II. Section III gives the formulation of the problem. Stationary waves induced by end walls are analyzed in Sec. IV. Both self-sustained transverse waves

due to global and absolute instabilities and mixed absolute-global oblique wave instabilities are considered in Sec. V. A comparison with experimental results is done in Sec. VI. A summary and concluding remarks are given in Sec. VII.

II. THEORETICAL BACKGROUND

A. On the conventional theory

The approach of Smith and Davis [1] is based on conventional linear stability theory. Unfortunately, predictions of this theory about the stability of spatially extended systems are often interpreted incorrectly by ignoring the distinction between the concepts of convective and absolute instabilities [9]. Therefore, it might be useful to recall some principal ideas underlying the linear stability analysis of spatially extended homogeneous systems. Our aim here is to present the necessary background in a physically obvious way, avoiding the mathematical complexities as much as possible. Our approach differs in some points from the commonly adopted one.

The basic state, whose stability is to be investigated, is assumed to be both stationary and uniform in one or more spatial directions. The equations governing the spatiotemporal evolution of infinitesimal perturbations of such a basic state are linear and independent of both time and the coordinates of which the basic state is independent. A particular solution of such equations is an exponential function of both time and the corresponding coordinates.

If the system is regarded as unbounded along the extended directions, there are no boundary conditions to be satisfied along those coordinates. Then an exponential variation of the perturbation along these coordinates may be arbitrary. This ambiguity may be eliminated by requiring the perturbation to be bounded at both infinities of the corresponding coordinates. This restricts the perturbation to a constant amplitude harmonic wave, called the Fourier mode $\psi \sim e^{i(\mathbf{k}\cdot\mathbf{r}-\omega t)}$, where $\mathbf{k}$ is a real wave vector having components only along those directions in which the basic state is uniform; $\mathbf{r}$ is the radius vector; and ω is a complex frequency, where $\omega_r = \mathcal{R}[\omega]$ is the oscillation frequency, but $\omega_i = \mathcal{I}[\omega]$ is the temporal growth rate of the corresponding perturbation. The frequency ω and wave vector $\mathbf{k}$ are constrained to satisfy the dispersion relation $D(\omega,\mathbf{k};R)=0$, where R stands for one or more parameters defining the problem. The dispersion relation may be regarded as implicitly defining ω as a function of argument $\mathbf{k}$ and parameter R: $\omega=\omega(\mathbf{k};R)$. Note that ω may in general be a multivalued function of $\mathbf{k}$. Further, ω will be used to denote the complex frequency branch having the largest imaginary part.

To determine whether the given basic state is stable or not, formally one has to investigate the evolution of all virtual perturbations. But as long as the problem is linear, an arbitrary disturbance may be considered as a superposition of independently evolving Fourier modes. According to this idea, after a sufficiently long time the perturbation will be dominated by the Fourier mode having the highest temporal growth rate $\omega_{i,c}=\omega_i(\mathbf{k}_c)$, where $\mathbf{k}_c$ is the critical wave vector at which this maximum is attained. It is said that the system is stable if $\omega_{i,c}<0$, but unstable if $\omega_{i,c}>0$.

However, it must be realized that this criterion may be ambiguous with respect to extended systems. The ambiguity stems from the double infinite limit used in deducing this criterion. Considering a single Fourier mode which extends over the whole space, one actually proceeds first to the limit of infinite space, and subsequently to the limit of infinite time $t\to\infty$. The problem one should be aware of is that the obtained result can depend on the order in which these limits are proceeded.

To illustrate this, consider a one-dimensional example of a spatially localized initial perturbation given by the wave packet

$$\psi_0(x)\sim e^{-(\varepsilon x/2)^2}e^{ik_c x},$$

where wave number k_c is that of the Fourier mode having maximum temporal growth rate, and ε defines the width of the wave packet. The limit $\varepsilon\to 0$ recovers the pure Fourier mode. In the wave-number space, this perturbation is given by the Gaussian distribution centered about k_c,

$$\tilde{\psi}_0(k)\sim \frac{1}{\varepsilon\sqrt{\pi}}e^{-[(k-k_c)/\varepsilon]^2}.$$

The evolution of this perturbation is given by the Fourier integral

$$\psi(x,t)\sim \int_{-\infty}^{\infty}\tilde{\psi}_0(k)e^{i(kx-\omega t)}dk. \tag{1}$$

If the width of the wave packet exceeds the wavelength ($\varepsilon \ll k_c$) considerably, the perturbation is significantly different from zero only for wave numbers sufficiently close to k_c. Then ω may be approximated by a power-series expansion

$$\omega(k)\approx \omega_c+\omega_k(k-k_c)+\frac{\omega_{kk}}{2}(k-k_c)^2, \tag{2}$$

where $\omega_c=\omega(k_c)$, $\omega_k=\partial\omega/\partial k|_{k=k_c}=\partial\omega_r/\partial k|_{k=k_c}$, and $\omega_{kk}=\partial^2\omega/\partial k^2|_{k=k_c}$. Note that the maximum of temporal growth rate at $k=k_c$ implies $\partial\omega_i/\partial k|_{k=k_c}=0$ and $\gamma_{kk}=\mathcal{I}[\omega_{kk}]<0$. Substituting Eq. (2) into Eq. (1), and taking the integral, we obtain

$$\psi(x,t)\sim \exp\left[-\frac{(x-\omega_k t)^2}{4\varepsilon^{-2}+2i\omega_{kk}t}\right]e^{i(k_c x-\omega_c t)}.$$

Note that this result is exact only when the dispersion relation coincides with the given power-series expansion. For the purpose of illustration, this is assumed to be the case here.

There are two distinct possibilities of how to evaluate the long-time asymptotics of the above solution. Proceeding first to the limit of infinite length of wave packet ($\varepsilon\to 0$), we recover the result of the conventional theory which yields $\omega_{i,c}$ for the temporal growth rate. The other possibility is to keep ε fixed and to proceed first to the limit $t\to\infty$. This results in the following asymptotic growth rate:

$$\omega_i(U)=\omega_{i,c}+\frac{\gamma_{kk}}{2|\omega_{kk}|^2}(\omega_k-U)^2,$$

where U is the translation velocity of the frame of reference where the wave packet is observed. Because $\gamma_{kk}<0$, this

temporal growth rate is in general lower than the conventional one, except for the frame of reference moving with the group velocity of the wave packet $U=\omega_k$, where both quantities coincide. Since the length of any real disturbance is always limited by that of the system, the last result gives the actual asymptotic growth rate for real systems.

Thus, just beyond the threshold predicted by the conventional theory, the most dangerous perturbation grows only in the frame of reference traveling with the group velocity of this perturbation, while it decays in any other frame of reference. This means that beyond this threshold the system is just able to amplify the disturbances excited externally. Such a behavior, actually predicted by the conventional analysis, is referred to as the convective instability. Since the most unstable perturbation grows only while it travels with respect to the laboratory frame of reference, the disturbances having a sufficiently small initial amplitude may leave the system of finite length before attaining an experimentally observable magnitude.

B. Global instability

An unstable small initial perturbation can attain an observable magnitude if it does not move away from the point of its excitation. This corresponds to the absolute instability which, however, is not the only possibility for the development of a self-sustained instability. Such an instability could develop directly beyond the threshold of convective instability if there were some feedback in the system redirecting a part of a growing perturbation back to the point of its origin. In principle, the needed feedback could be provided by coupling between different Fourier modes, but from the point of view of the conventional linear theory there is none. However, this is not always so. The principal point to realize is that the mutual independence of different traveling waves is not only due to the linearity of the problem, but also stems from the assumed absence of lateral boundaries. For a real bounded system there are certain conditions which must be satisfied at the lateral walls. The time-independent boundary conditions cannot be satisfied by a single traveling wave. Rather, a superposition of several traveling waves is required. Therefore, different traveling waves, which would be mutually independent in an unbounded system, become coupled in the presence of confining walls.

Since the boundary corrupts the uniformity of the basic state necessary for propagation of a single Fourier mode, while preserving its time invariance, reflection of a single wave may result in all modes permitted by the dispersion relation at the frequency of the incident wave. To find reflected waves, we have to solve the dispersion relation for complex wave numbers at real frequencies. This problem is equivalent to that of finding the spatial evolution of a free wave apart from the source forcing it with the given frequency. Complex wave numbers mean that a perturbation may be either attenuated or amplified by the medium. The problem of distinguishing between these two opposite cases will be addressed in Sec. II C.

As argued above, a single incident wave may be coupled to multiple reflected waves. If the system is extended enough, the reflected waves sufficiently far away from the boundary will be dominated by the mode having either the highest amplification or minimal attenuation rate. Subsequently this will be referred to as the highest spatial growth rate. To derive the dispersion relation for an extended but bounded system, consider a wave sufficiently far away from the confining boundaries and propagating in the positive direction of the x axis,

$$\psi_0(x,t)=Ae^{i(k_+x-\omega t)}, \tag{3}$$

where A is the amplitude of the wave, and $k_+=k_+(\omega;R)$ is the complex wave number having the largest spatial growth rate for the given frequency ω and control parameter R. Suppose that the wave with the highest spatial growth rate propagating in the opposite direction at the same frequency and control parameter has the complex wave number $k_-=k_-(\omega;R)$. Because within the framework of linear theory the amplitude of the reflected wave must be proportional to that of the incident wave, the dominating mode excited by reflection of the incident wave ψ_0 from the boundary at $x=L$ is given by

$$\psi_1(x,t)=\mathcal{R}_1Ae^{ik_+L}e^{i(k_-(x-L)-\omega t)},$$

where $\mathcal{R}_1$ is a complex, generally unknown reflection coefficient. The wave reflected once more from the opposite boundary at $x=0$ may be written as

$$\psi_2(x,t)=\mathcal{R}_1\mathcal{R}_2Ae^{i(k_+-k_-)L}e^{i(k_+x-\omega t)}, \tag{4}$$

where $\mathcal{R}_2$ stands for the corresponding reflection coefficient. For a superposition of two waves to evolve exponentially in time with the given complex frequency ω (to be a normal mode), it is necessary that the twice reflected wave (4) coincides with the incident one (3). This yields the dispersion relation for the system of large but finite length L [10],

$$\mathcal{R}_1\mathcal{R}_2e^{i(k_+-k_-)L}=1. \tag{5}$$

The imaginary part of Eq. (5), implying

$$\mathcal{R}[k_+(\omega;R)-k_-(\omega;R)]L=-\arg(\mathcal{R}_1\mathcal{R}_2)\pm m\pi,$$
$$m=0,2,4,\ldots, \tag{6}$$

defines a discrete spectrum of wave numbers which tends to be continuous as $L\to\infty$. Thus, in the limit of an infinitely extended system, the above relation is satisfied by any wave numbers $k_\pm$, and the dispersion relation actually reduces to the real part of Eq. (5) alone which in addition significantly simplifies by getting independent of both the unknown reflection coefficients $\mathcal{R}_1$, $\mathcal{R}_2$ and the length L,

$$\mathcal{I}[k_+(\omega;R)-k_-(\omega;R)]=0. \tag{7}$$

Thus the dispersion relation for an extended, bounded system, which is originally due to Kulikovskii [11], is defined in terms of the dispersion relation of the corresponding unbounded one. Note that by increasing the length of the system this dispersion relation does not in general proceed to that of the equivalent unbounded system. An exception is for mirror-symmetric systems satisfying $k_\pm=\pm k(\omega;R)$, for which the convective instability also automatically ensures the global one [11]. In general, the threshold of the global instability is higher than that of the convective instability beyond which a spatially amplified wave necessary for glo-

bal instability can arise [12]. It is interesting to note that, although the absolute instability does not require reflections from the lateral walls, it appears just as a special case of the global one when both waves constituting the global mode merge together at some wave number $k_0 = k_+ = k_-$.

C. Propagation direction in an active medium

The concept of global instability essentially relies on the criterion defining the direction of wave propagation. It is well known that for an active (nonconservative) medium contrary to a conservative one the group velocity does not in general present such a criterion [13]. The problem of identifying the direction of propagation is equivalent to that of distinguishing between spatially amplified and attenuated waves. Since the space contrary to the time permits evolution of waves in either direction, the sign of the imaginary part of the wave number, unlike that of the temporal growth rate, cannot be used to discriminate those two opposite cases.

A general criterion for distinguishing spatially amplified and attenuated waves has been proposed by Twiss [14] (see also Ref. [10]). This criterion can be interpreted as follows. Consider a free wave having a temporally constant, but in general spatially varying, amplitude. If there is no absolute instability, such a wave must be due to some remote forcing rather than being self-sustained. According to the causality principle, it must take a finite time for the perturbation to propagate from the source of its excitation to the point where it is observed. Forcing can be increased so quickly that the amplitude of the waves close to the source becomes larger than the amplitudes of those sufficiently far away which have been emitted earlier, when the forcing was lower. An arbitrary fast increase of forcing may be accomplished exponentially with sufficiently high temporal growth rate ω_i. Consequently, for $\omega_i \to \infty$ all waves must be evanescent with distance away from the source. To determine whether the given wave is spatially amplified or attenuated one needs to increase ω_i while following the change of k_i. Change of sign of k_i as $\omega_i \to \infty$ indicates that the wave has originally been spatially amplified. Otherwise, it has been an attenuated one. The direction of propagation can straightforwardly be deduced from the sign of k_i. Although such a procedure is sufficient for determining the direction of propagation, it may not always be necessary. In a number of cases of practical significance a simpler criterion may be used, which in contrast to the previous one is local in the complex frequency plane and, therefore more convenient for practical application [15]. Such a criterion is suggested by the following causality arguments.

Because the problem for small-amplitude perturbations, which are assumed to be the case here, is linear, the amplitude of such waves must be proportional to that of the forcing. When the latter is changed, the same must happen with the former. According to the causality, variation of the perturbation must propagate from the source of its excitation rather than take place immediately in the whole space. To determine the direction of propagation, suppose that for a constant amplitude forcing there is a wave generated with the spatially varying amplitude at rate $k_i = \mathcal{I}[k]$. If the forcing is changed exponentially with a small temporal growth rate $\delta\omega_i$, the spatial growth rate changes by δk_i. This corresponds to the change of the amplitude of the original wave by factor $C(x,t) = e^{-(\delta k_i x - \delta\omega_i t)}$. From here it follows that the point of constant amplitude $C = \text{const}$ moves with velocity

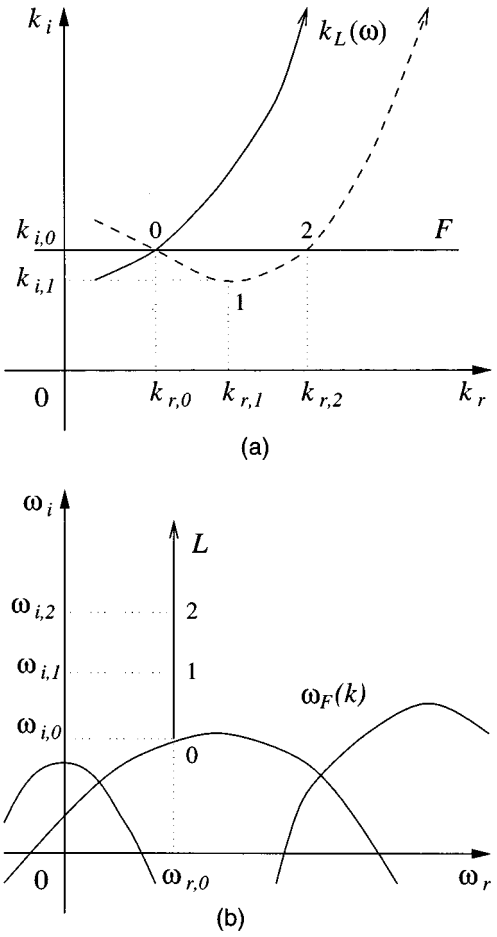

FIG. 1. Mappings between complex wave number (a) and frequency planes (b).

$$U = \frac{\delta\omega_i}{\delta k_i} = \left(\frac{\partial\omega_i}{\partial k_i}\right)_{\omega_r = \text{const}}.$$

Since k is a complex function of complex argument ω, we obtain

$$U = \mathcal{R}\left(\frac{dk}{d\omega}\right)^{-1} = \mathcal{R}\left(\frac{d\omega}{dk}\right)^{-1}\left|\frac{d\omega}{dk}\right|^2. \tag{8}$$

Thus U coincides with the group velocity when the latter is real. But, in general, U has the same sign as that of the real part of the group velocity. Since the suggested criterion in contrast to the conventional one is defined by a local relation between complex frequency and wave number, both criteria are not necessarily equivalent. This raises the question about the correspondence between both criteria which is addressed below.

Consider a solution of the dispersion relation mapping contour F, which passes in the complex wave number plane at fixed k_i parallel to the real axis, onto the complex frequency plane (see Fig. 1). Assume that for every bounded

spatial growth rate $|k_i|<K$ the temporal growth rates are bounded from above $\omega_i<\Omega$, where K and Ω are some finite constants. Note that this constraint is implied by the causality principle which must be obeyed by any reasonably posed problem. The statement we want to prove is

$$\operatorname{sgn} \mathcal{R}\left(\frac{d\omega}{dk}\right)=\operatorname{sgn}(k_i)_{\omega_i\to\infty}. \tag{9}$$

for the branch of complex frequency having largest temporal growth rate ω_i at the given frequency ω_r and spatial growth rate k_i. First, by the same arguments which led to relation (8), we obtain

$$\operatorname{sgn} \mathcal{R}\left(\frac{d\omega}{dk}\right)=\operatorname{sgn}\left(\frac{\partial k_i}{\partial \omega_i}\right).$$

Let us focus here on the complex frequency branch which for the waves with spatial growth rate $k_{i,0}$ has at frequency $\omega_{r,0}$ the highest temporal growth rate $\omega_{i,0}$. Now, increase ω_i above $\omega_{i,0}$, upon keeping $\omega_r=\omega_{r,0}$ fixed, and follow variation of the corresponding solution of the dispersion relation in the complex wave number plane. The assumed constraint $\omega_i<\Omega$ for all $|k_i|<K$ implies that $k_i\to\infty$ as $\omega_i\to+\infty$. Suppose that the statement to be proved is false,

$$\operatorname{sgn}\left(\frac{\partial k_i}{\partial \omega_i}\right)_{\omega_i=\omega_0}\neq \operatorname{sgn}(k_i)_{\omega_i\to\infty}. \tag{10}$$

This implies that with increasing ω_i slightly above $\omega_{i,0}$, the corresponding k_i proceeds away from its asymptotic value $k_{i,\infty}=k_i|_{\omega_i\to\infty}$. Thus at some $\omega_{i,1}>\omega_{i,0}$ there must be such $k_{i,1}$ lying on the opposite side from $k_{i,0}$ than $k_{i,\infty}$, *i.e.*, $|k_{i,1}|<|k_{i,0}|<|k_{i,\infty}|$. For $k_{i,1}$ to proceed to $k_{i,\infty}$, as ω_i is increased further from ω_1 to $+\infty$, there must be such $\omega_{i,2}>\omega_{i,1}>\omega_{i,0}$ at which $k_{i,2}=k_{i,0}$. This means that for the given $k_{i,0}$ there is another branch in the complex frequency plane having a temporal growth rate $\omega_{i,2}>\omega_{i,0}$ at the frequency $\omega_{r,0}$. However, this contradicts our basic premise that $\omega_{i,0}$ is the highest temporal growth rate for the given frequency $\omega_{r,0}$ and spatial growth rate $k_{i,0}$. Consequently, assumption (10) is false, which proves relation (9). Note that this proof concerns only the wave branch having the highest growth rate at the given frequency and spatial growth rate.

III. PROBLEM DEFINITION

Consider a horizontal layer of liquid of kinematic viscosity ν, density ρ, thermal expansion coefficient α, and thermal conductivity κ. The layer, having at rest depth d, is bounded from below by a plane perfectly thermally insulating or conducting plate, and above by a free surface characterized by thermal conductance per unit area h. A constant temperature gradient β is imposed along the layer, and a steady shear flow is set up by a combined effect of buoyancy and viscous surface stress due to the temperature dependence of surface tension assumed to vary according to the linear law

$$\tau=\tau_0-\gamma(T-T_0). \tag{11}$$

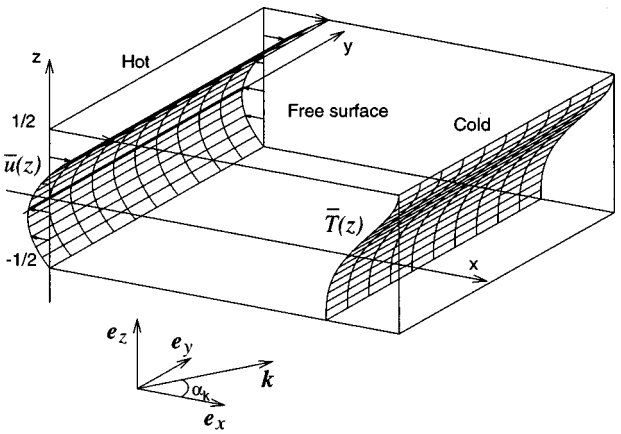

FIG. 2. Sketch of the formulation of the problem.

Here $\gamma=-d\tau/dT>0$ denotes the negative rate of change of surface tension with temperature, while τ_0 and T_0 are reference values for surface tension and temperature, respectively. The layer is assumed to be extended enough so that a homogeneous basic flow could develop sufficiently far away from the lateral walls. A sketch of the problem is shown in Fig. 2. The origin of the Cartesian coordinate system used is set at the midheight of the layer. The x axis is directed against to the imposed temperature gradient β, and the z axis is normal to the plane of the layer. The surface tension is assumed to be high enough so that the free surface may be considered as a planar and nondeformable boundary.

Transforming both the governing equations and boundary conditions to a dimensionless form, the depth d is chosen as a length scale, and the time t, velocity field $\mathbf{v}$, pressure field p, and temperature difference $T-T_0$ are referred to scales d^2/ν, ν/d, $\rho\nu^2/d^2$, and βd, respectively. The fluid flow is governed by the Navier-Stokes equation, the incompressibility constraint, and the energy equation:

$$\partial_t\mathbf{v}+(\mathbf{v}\cdot\boldsymbol{\nabla})\mathbf{v}=-\boldsymbol{\nabla}p+\nabla^2\mathbf{v}+\mathrm{Gr}T\mathbf{e}_z, \tag{12}$$

$$\boldsymbol{\nabla}\cdot\mathbf{v}=0, \tag{13}$$

$$\partial_t T+\mathbf{v}\cdot\boldsymbol{\nabla}T=\mathrm{Pr}^{-1}\nabla^2 T, \tag{14}$$

where $\mathrm{Pr}=\nu/\kappa$ is the Prandtl number and $\mathrm{Gr}=\alpha\beta g d^4/\nu^2$ is the Grashof number characterizing the effect of buoyancy.

At the free surface $z=\frac{1}{2}$ there is balance of thermocapillary and shear stresses,

$$\mathbf{e}_z\times(\partial_z\mathbf{v}+\mathrm{Re}\ \boldsymbol{\nabla}T)=\mathbf{0}, \tag{15}$$

and a kinematic constraint resulting from the nondeformability assumption $\mathbf{e}_z\cdot\mathbf{v}=0$, where $\mathrm{Re}=\gamma\beta d^2/\rho\nu^2$ is the Reynolds number which defines the strength of the thermocapillary effect. In order to keep consistency with previous papers on the given subject we introduce additionally the Marangoni number $\mathrm{Ma}=\mathrm{Re}\,\mathrm{Pr}$ which is not an independent parameter here. Besides, it is more convenient to use the dynamic Bond number $\mathrm{Bo}=\mathrm{Gr}/\mathrm{Re}=g\alpha\rho d^2/\gamma$ instead of Gr to define the relative effect of buoyancy.

Between the free surface and the surrounding medium there is a heat transfer which, as usually, is assumed to obey Newton's law

$$\partial_z T = -\mathrm{Bi}(T - T_\infty(x)) \quad \text{on} \quad z = \tfrac{1}{2}, \tag{16}$$

where $\mathrm{Bi} = hd/\kappa$ is the Biot number and $T_\infty(x) = -x$ is the temperature of the surrounding medium, having the same imposed temperature gradient as the liquid layer. On the rigid bottom there are no slip, impermeability, and zero heat flux (insulating bottom)

$$\mathbf{v} = \mathbf{0}, \quad \partial_z T = 0 \quad \text{on} \quad z = -1/2,$$

or a fixed temperature (perfectly conducting bottom)

$$T(-1/2) = T_\infty(x) = -x.$$

The problem under consideration has a steady parallel flow solution $\overline{\mathbf{v}} = (\overline{u}, 0, 0)$, maintaining zero mass flux through any vertical cross section

$$\overline{u}(z) = \mathrm{Re}\left[\frac{3z^2}{4} + \frac{z}{4} - \frac{1}{16} - \mathrm{Bo}\left(\frac{z^3}{6} - \frac{z^2}{16} - \frac{z}{16} + \frac{1}{192}\right)\right], \tag{17}$$

$$\begin{aligned}\overline{T}(x,z) = -x - \mathrm{Pr}\ \mathrm{Re}\Bigg\{&\frac{z^4}{16} + \frac{z^3}{24} - \frac{z^2}{32} - \left(1 - \frac{2S}{3}\right)\frac{z + 1/2}{32} \\ &+ \frac{P}{3} - \mathrm{Bo}\left[\frac{z^5}{120} - \frac{z^4}{192} - \frac{z^3}{96} + \frac{z^2}{384}\right. \\ &\left. + \left(1 + \frac{3S}{5}\right)\frac{z + 1/2}{192} + \frac{P}{20}\right]\Bigg\},\end{aligned} \tag{18}$$

$$\overline{p}(x,z) = \mathrm{Re}\left[x\left(\frac{3}{2} + \frac{\mathrm{Bo}}{8}\right) + \mathrm{Bo}\int \overline{T}(x,z)\,dz\right], \tag{19}$$

where $S = 0$ and $P = 23/16^2$ for the thermally insulating bottom, and $S = \mathrm{Bi}/(1 + \mathrm{Bi})$ and $P = 7/16^2$ for the conducting bottom.

We analyze the linear stability of the basic states (17)–(19) with respect to the infinitesimal disturbances in the form

$$(\mathbf{v}, p, T) = (\overline{\mathbf{v}}, \overline{p}, \overline{T}) + \{\hat{\mathbf{v}}(z), \hat{p}(z), \hat{T}(z)\}\exp[i(\mathbf{k}\cdot\mathbf{r} - \omega t)], \tag{20}$$

where $\mathbf{k} = (k_x, k_y)$ is the wave vector coplanar to the layer, $\mathbf{r}$ is the radius vector, but λ is a complex temporal growth rate. Upon elimination of the pressure, the disturbance equations may be written as

$$\mathbf{D}^2[\mathbf{D}^2 + i\omega]\hat{w} - ik_x[\overline{u}\mathbf{D}^2 - \overline{u''}]\hat{w} + \mathrm{Bo}\ \mathrm{Re}\ \hat{T} = 0, \tag{21}$$

$$[\mathbf{D}^2 + i\omega]\hat{u} - ik_x\overline{u}\hat{u} - k_y\overline{u'}\hat{w} = 0, \tag{22}$$

$$[\mathrm{Pr}^{-1}\mathbf{D}^2 + i\omega - ik_x\overline{u}]\hat{T} - \overline{T'}\hat{w} + k^{-2}(ik_x\hat{w}' + k_y\hat{u}) = 0, \tag{23}$$

where $\mathbf{D}^2 \equiv [(d^2/dz^2) - k^2]$ and the prime denotes the derivative with respect to z, $\hat{w} = \mathbf{e}_z\cdot\hat{\mathbf{v}}$ is the vertical velocity, and $\hat{u} = (\mathbf{k}\times\mathbf{e}_z)\cdot\hat{\mathbf{v}}$ is further referred to as the longitudinal velocity. It means that we consider the velocity disturbances in the coordinate system linked with the direction of the wave vector.

The boundary conditions for the vertical velocity $\hat{w}$ are

$$\hat{w}'' + k^2\ \mathrm{Re}\ \hat{T} = 0 \quad \text{on} \quad z = \tfrac{1}{2}, \tag{24}$$

$$\hat{w}'(-\tfrac{1}{2}) = \hat{w}(\pm\tfrac{1}{2}) = 0. \tag{25}$$

For the longitudinal velocity component, we have

$$\hat{u}'(\tfrac{1}{2}) = \hat{u}(-\tfrac{1}{2}) = 0. \tag{26}$$

The boundary conditions for the temperature perturbation are

$$\hat{T}' + \mathrm{Bi}\hat{T} = 0 \quad \text{on} \quad z = \tfrac{1}{2} \tag{27}$$

at the free surface, and

$$\hat{T}'(-\tfrac{1}{2}) = 0 \quad \text{or} \quad \hat{T}(-\tfrac{1}{2}) = 0 \tag{28}$$

at insulating or conducting bottoms, respectively. Since thermal boundary conditions have mostly a quantitative effect, which may be very significant for small Pr [16], the following results will be presented only for both free surface and bottom being adiabatically insulated boundaries, i.e., $\mathrm{Bi} = 0$ and $\hat{T}'(-\tfrac{1}{2}) = 0$.

The dispersion relation is approximated by making use of a modified Chebyshev tau spectral method [17], leading to a matrix eigenvalue problem [18]. Spatial branches $k(\omega_0)$ are formally defined by a polynomial matrix eigenvalue problem with respect to k. It is more advantageous to seek spatial branches as solutions of the complex equation $\omega(k) - \omega_0 = 0$, where $\omega(k)$ are complex frequencies defined by the ordinary matrix eigenvalue problem.

IV. STATIONARY CELLS DUE TO THE END WALLS

The uniformity of the basic state may be disturbed by the lateral walls. In this section we consider how far the influence of these walls can extend into the homogeneous basic state. The disturbance caused by lateral walls has two specific features. The first is a relatively large amplitude. If this perturbation is evanescent with the distance, which is assumed to be the case here in order to allow for the development of the spatially uniform basic state, then sufficiently far away from the boundary the amplitude becomes small enough for the linear theory to be applicable. The second specific feature is the stationarity of this perturbation. Thus the sought penetration distance is given by the inverse of the spatial attenuation rate of the zero-frequency mode.

Such an approach was used originally by Bye [19], who considered the problem of a steady flow in a rectangular basin driven by a horizontal wind causing a constant shear stress at the free surface of the liquid. The same problem was reconsidered also in Ref. [20] in the context of thermocapillary convection of a zero Prandtl number liquid. In this approximation, perturbations of temperature and flow fields are decoupled. As a result, the problem considerably simplifies by reducing to a single equation (21). The boundary condition (24) is replaced by the fixed-stress condition

$$\hat{w}'' = 0 \quad \text{on} \quad z = \tfrac{1}{2}. \tag{29}$$

Complex wave numbers for a stationary perturbation are found from the equation $\omega(k; \mathrm{Re}) = 0$, which has an infinite number of discrete roots. We are interested only in the mode

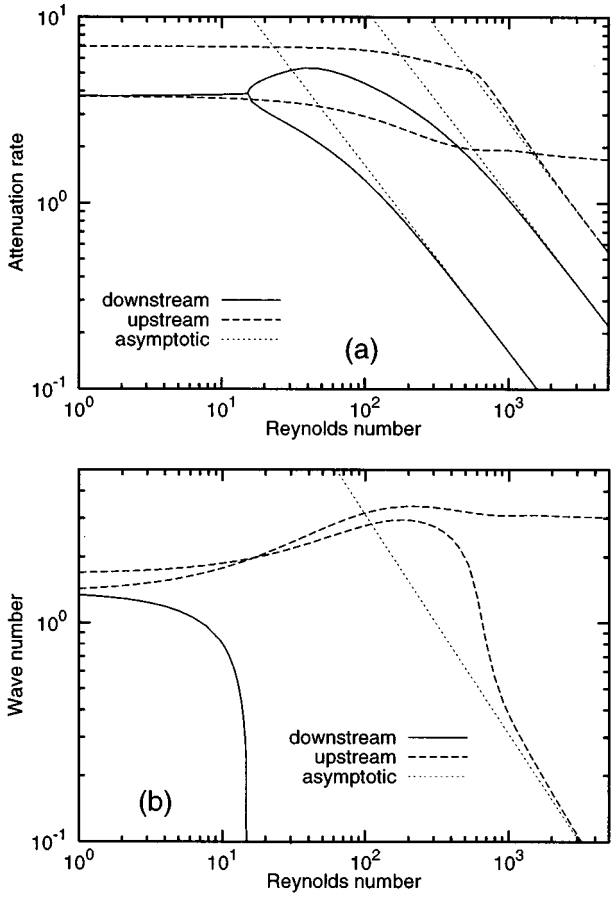

FIG. 3. Dimensionless spatial attenuation rates (a) and wave numbers (b) of purely hydrodynamic (Pr=0) upstream and downstream dominating wave modes vs the Reynolds number for the surface-tension-driven basic flow (Bo=0).

with the largest spatial growth rate which dominates the perturbation far away from the wall. There is one such mode propagating downstream and one upstream. Further, let us examine how these perturbations vary with the Reynolds number. In the limit Re=0, Eq. (21) reduces to $\mathbf{D}^2[\mathbf{D}^2+i\omega]\hat{w}=0$ which for $\omega=0$ has nontrivial solutions satisfying the boundary conditions (25) and (29) only when $k=k_x$ satisfies the dispersion relation $\sinh(2k)-2k=0$ [20]. This equation has an infinite number of discrete roots which are not only complex conjugate, but also symmetric by pairs with respect to the imaginary axis. From the physical point of view it is obvious that such viscosity-dominated waves corresponding to the complex wave numbers must be evanescent.

The advection of disturbances by the basic flow appearing at nonzero Reynolds numbers breaks the symmetry between the waves propagating in different directions. Since the advection has no effect on the longitudinal disturbances ($k_x=0$) caused by the sidewalls, the following analysis will be concerned with the transverse disturbances due to the end walls only. Let us consider first the basic flow driven solely by the gradient of surface tension. It may be seen in Fig. 3 that the spatial attenuation rates of the two dominating perturbations induced by the hot and cold end walls, and propagating downstream and upstream relative to the surface velocity, respectively, decrease with increase of the Reynolds number. However, it is important to notice that these perturbations remain spatially attenuated regardless of how large the Reynolds number is. This implies that the basic flow under consideration is hydrodynamically stable with respect to at least zero-frequency disturbances. A more detailed examination shows that the basic flow driven solely by the surface tension is linearly stable with respect to purely hydrodynamic perturbations of any frequency [18]. It is important to notice in Fig. 3 that for sufficiently large Re complex wave numbers depend asymptotically on the Reynolds number as $k\sim \mathrm{Re}^{-1}$. This means that for $\mathrm{Re}\gg 1$ both wavelength and attenuation distance increase proportionally with Re.

Let us turn further to a more detailed examination of the limit $\mathrm{Re}\to\infty$. In this case, it is advantageous to rescale the wave number as

$$k=\tilde{k}\ \mathrm{Re}^{-1}. \tag{30}$$

Equation (21) then reduces to

$$\frac{d^2}{dz^2}\left[\frac{d^2}{dz^2}+i\omega\right]\hat{w}-i\tilde{k}_x\left[\tilde{u}\,\frac{d^2}{dz^2}-\tilde{u}''\right]\hat{w}=0, \tag{31}$$

where $\tilde{u}(z)=\mathrm{Re}^{-1}\,\overline{u(z)}$. The asymptotic growth rates found by making use of this reduced formulation are seen in Fig. 3 to recover quite well the exact solution as $\mathrm{Re}\to\infty$.

The spatial evolution of perturbations can change principally when nonzero Prandtl numbers are considered. In this case, the flow disturbances become coupled with those of temperature which are governed by Eq. (23). For the transverse disturbances under consideration the hydrodynamic part of the problem is still posed by Eq. (21). The sole feedback of the temperature perturbation to that of the flow is provided by the boundary condition (24).

Temperature perturbations are associated with additional wave branches which, in the limit $\mathrm{Re}\to 0$, are decoupled from the hydrodynamic ones considered above. When both the free surface and the bottom are adiabatic boundaries defined by the boundary conditions (27) and (28), with Bi=0, it can readily be found from Eq. (23) that in the limit $\mathrm{Re}\to 0$ the wave numbers of the dominating perturbations are $k_{\pm}=\pm i\pi$. For nonzero Re the hydrodynamic and thermal modes are no longer independent. As seen in Fig. 4, where dominating spatial attenuation rates versus Re are plotted for Pr=0.01, an increase of Re can lead to the merging of different modes. However, note that large-Re asymptotics of spatial branches for small but nonzero Pr and Pr=0 are different. This difference is due to the effect of the basic flow on the temperature disturbances, which is completely absent for Pr=0. Conversely, for small but nonzero Pr, a sufficiently large Re can be attained at which the effect of advection of temperature perturbations ($\sim$Pr Re) becomes significant. As seen in Fig. 4, for a finite Prandtl number (Pr=0.01) and sufficiently large Re the downstream wave branch becomes spatially oscillating like the upstream one. But a more important result evident in Fig. 4 is that the asymptotics of wave number $k\sim \mathrm{Re}^{-1}$ also holds for nonzero Pr. Therefore, similarly as for Pr=0, let us make use of the rescaled wave number $\tilde{k}$, Eq. (30), and rescale additionally

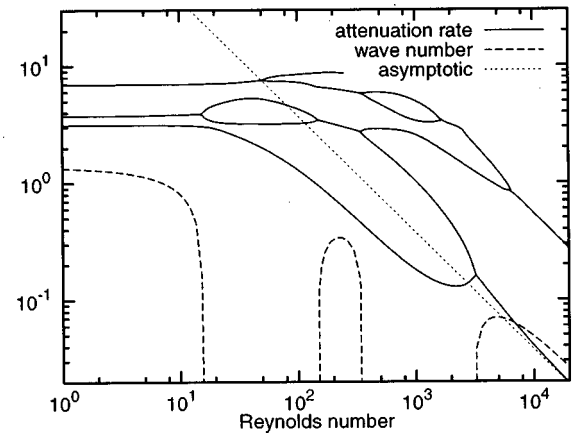

FIG. 4. Dimensionless spatial attenuation rates and wave numbers of the downstream dominating wave modes vs the Reynolds number for the surface-tension-driven basic flow (Bo=0) at Pr=0.01.

the temperature perturbation as $\hat{T}=\mathrm{Re}\,\hat{\theta}$. Substituting the rescaled temperature into Eq. (23) and proceeding to the limit Re$\to\infty$, we obtain

$$\left[\mathrm{Pr}^{-1}\frac{d^2}{dz^2}+i\omega-i\tilde{k}_x\tilde{u}\right]\hat{\theta}=\tilde{T}'\hat{w}-\tilde{k}^{-2}(i\tilde{k}_x\hat{w}'+\tilde{k}_y\hat{u}), \tag{32}$$

where $\tilde{T}'(z)=\mathrm{Re}^{-1}\,\overline{T'}(z)$. In terms of $\tilde{k}$ and $\hat{\theta}$, the boundary condition (24) reads

$$\hat{w}''+\tilde{k}^2\hat{\theta}=0 \quad \text{on } z=\tfrac{1}{2}. \tag{33}$$

Equations (31) and (32) together with boundary conditions (25), (27), (28), and (33) rewritten in terms of $\hat{\theta}$ pose the problem for asymptotic spatial branches at finite Pr as Re$\to\infty$.

As seen in Fig. 5, where the asymptotic downstream attenuation rate is plotted versus Pr, the coupling of the flow and the temperature perturbations can have a principally new effect. That is, the downstream attenuation rate decreasing with growth of Pr becomes negative for Pr$>$0.67, where the wave turns from a spatially attenuated to an amplified one. This means that the stationary perturbation induced by the hot end wall can spread downstream throughout the whole layer, experiencing no attenuation. This results in a stationary in time, but spatially oscillating, wave extending from the hot end wall over the whole layer.

At the point of zero spatial attenuation rate, where the wave turns from a spatially attenuated to an amplified one, the wave number becomes purely real. Additionally, the steady amplitude of the wave implies that the temporal growth rate is zero as well. Thus the given point lies on the conventional neutral stability curve defining the threshold of the convective instability which for the zero-frequency perturbation is given by the two conditions $\omega_i(k_s;\mathrm{Re}_s)=0$ and $\omega_r(k_s;\mathrm{Re}_s)=0$, where k_s is real. This pair of equations defines the critical Re_s beyond which a spatially amplified stationary wave pattern emerges, while k_s gives the corresponding wave number. The threshold of this instability depending on the Prandtl number is presented in terms of the critical

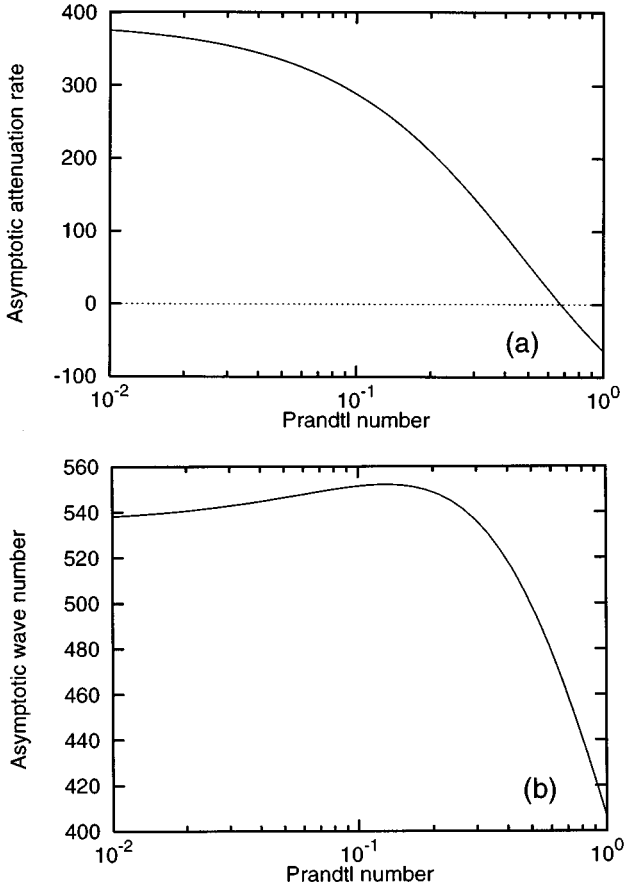

FIG. 5. Dimensionless downstream asymptotic attenuation rate (a) and the corresponding wave number (b) vs the Prandtl number for Re$\to\infty$ and Bo=0.

Marangoni number in Fig. 6. Note first that the stationary instability, like the oscillatory transverse wave, occurs only for sufficiently large Pr. Second, it is evident that the stationary perturbation is not convectively the most unstable one. There is a certain range of nonzero frequency modes which

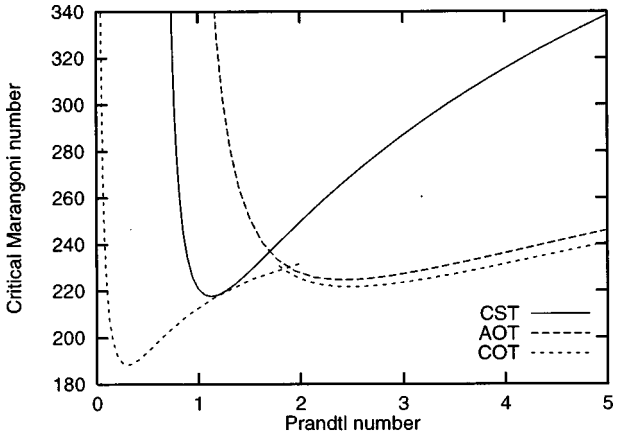

FIG. 6. Critical Marangoni numbers vs Prandtl number for various transverse wave instabilities of the thermocapillary-driven basic flow (Bo=0). CST, AOT, and COT stand for convective stationary, absolute oscillating, and convective oscillating transverse waves, respectively. The last (COT) is the threshold of the oscillatory convection predicted by the conventional theory.

become convectively unstable before the stationary one. However, these convectively unstable oscillating modes, contrary to the stationary one, may be experimentally unobservable. The principal difference between the stationary and oscillating modes is that the first is generated by a permanent, large-amplitude disturbance due to confining boundaries, whereas the latter are caused by random small-amplitude disturbances like noise. For such perturbations to be amplified by a convectively unstable medium up to an experimentally observable amplitude either the amplification rate or the length of system must be large enough [7].

V. SELF-SUSTAINED INSTABILITIES

A. Transverse waves

Here let us consider transverse disturbances ($k_y=0$) of the basic flow driven solely by the thermocapillary effect. The conventional linear stability analysis is concerned with neutrally stable constant amplitude Fourier modes defined by real wave numbers. As follows from the basic discussion, such waves may in general be not self-sustained. Consequently, they must be due to some remote forcing. If so, then each such wave has to be associated with the direction in which it leaves the source. Adopting such a point of view, we will look in the following for the conditions necessary for the development of self-sustained waves.

For this purpose it is advantageous to examine the neutral curves plotted in Fig. 7 showing the marginal Marangoni number for temporally neutral waves ($\omega_i=0$) versus the frequency of these waves. The curve with $k_i=0$ corresponds to the conventional stability threshold for constant amplitude waves. As is seen, the constant amplitude waves can propagate only when the Marangoni number exceeds a certain threshold, and the forcing frequency is not too high. For low enough frequencies the marginal Marangoni number is at least a double-valued function. Moreover, for each Marangoni number permitting propagation of constant amplitude waves there are at least two such waves which may be emitted at different frequencies of forcing. But the most important fact to notice is that the neutral curve makes a loop and at some point intersects itself, where the frequencies of both constant amplitude waves, which can propagate at the corresponding Marangoni number, coincide. Were these two waves propagating in the opposite directions, they might be coupled by reflections from the end walls, and, according to the global stability condition (7), they could sustain each other in a sufficiently extended liquid layer without aid of any external forcing.

To determine the direction of propagation of these waves, let us examine the variation of the neutral curve upon adding to the wave number a small imaginary part. The neutral curve for a complex wave number defines the marginal Marangoni numbers permitting propagation of the waves with a temporally steady, but spatially varying amplitude. It may be seen in Fig. 7(a) that for a nonzero spatial growth rate one branch of the neutral curve passes above the self-intersection for constant amplitude waves, while the other does it below that point. This allows us to deduce the sign of the real part of the group velocity of the corresponding waves. The neutral curves under consideration $\mathrm{Ma}=\mathrm{Ma}(\omega_r,k_i)$ are implicitly defined by the condition $\omega_i(\omega_r,k_i;\mathrm{Ma})=0$. By taking

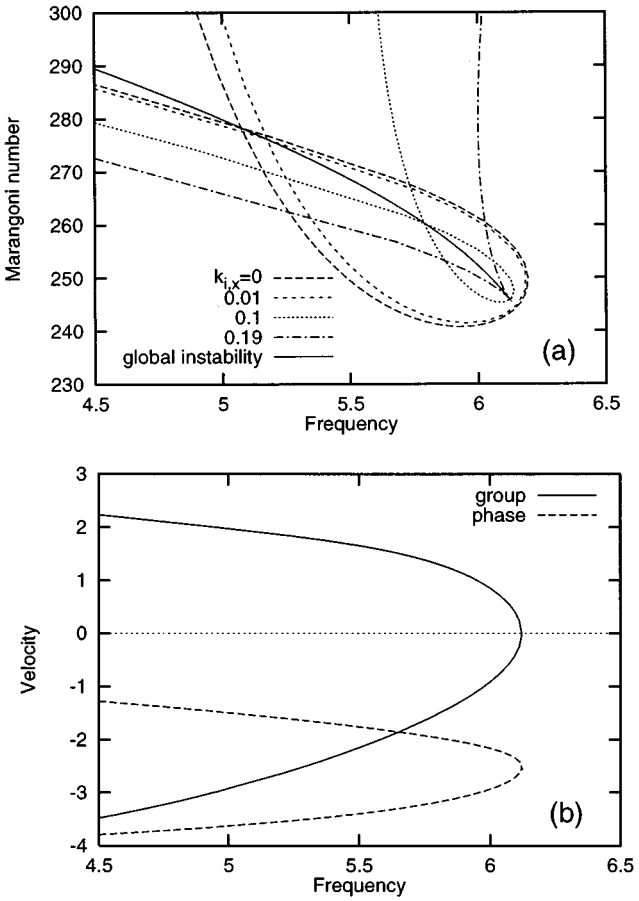

FIG. 7. Neutral curves for various spatial growth rates and the threshold of global instability given by self-intersections (a). Phase and group velocities vs frequency at the threshold of the global instability (b); Pr=5.

the partial derivative with respect to k_i of this condition, we obtain

$$\frac{\partial\omega_i}{\partial k_i}=-\frac{\partial\omega_i}{\partial\,\mathrm{Ma}}\frac{\partial\,\mathrm{Ma}}{\partial k_i}.$$

The sign of the term $\partial\omega_i/\partial\,\mathrm{Ma}$ depends on the direction of variation of the temporal growth rate as Ma crosses the neutral stability threshold. Since in the case under consideration the wave becomes temporally growing ($\omega_i>0$) as Ma rises above the neutral stability threshold, the corresponding term is positive. Thus the neutral curve proceeding downwards for $\delta k_i>0$ or upwards for $\delta k_i<0$ implies a negative real part of the group velocity. The opposite is true when the neutral curve proceeds upwards for $\delta k_i>0$ or downwards for $\delta k_i<0$. Concerning the conventional neutral stability threshold for constant amplitude waves the above criteria may be interpreted as follows. If, upon adding to the wave number a small imaginary part δk_i, the neutral stability threshold shifts to the region of temporally growing constant amplitude waves, the corresponding waves with $k_i=\delta k_i$ are spatially amplified rather than attenuated. Consequently, the two waves near the intersection have opposite signs of the real part of the group velocity. Note that we proved this sign to define the direction of propagation only for the wave having the highest temporal growth rate at the given frequency.

Thus this criterion is not granted to be correct for all other wave modes having lower temporal growth rates at the given frequency. However, there is one particular point on each curve plotted in Fig. 7(a), where the criterion of the group velocity certainly gives the correct direction of propagation for two wave branches. This is the point of self-intersection of the neutral curve, where the frequencies of both neutrally stable waves having the same spatial growth rate occur at the same Marangoni number. Since there are no other neutrally stable modes of this frequency and the given spatial growth rate at the Marangoni numbers below the intersection, this point corresponds to the maximal temporal growth rate for the given frequency and spatial growth rate. Thus, at the self-intersection, the criterion of the group velocity is valid for both branches of the neutral curve. The conclusion is that these two are indeed oppositely propagating waves which can therefore sustain each other by reflections from the confining end walls, giving rise to the global oscillatory instability.

A closer examination of the neutral curves shown in Fig. 7(a) reveals that there may be a global instability at Marangoni numbers lower than that for the constant amplitude waves. At sufficiently small positive spatial growth rate there is another self-intersection point of the corresponding neutral curve where one wave is amplified, but another attenuated at the same rate. The minimum of the global instability threshold occurs when the loop of the neutral curve tightens together to form a cusp, which is seen in Fig. 7(a) for $k_i = 0.19$. Since both waves merging at the cusp have opposite signs of the real part of the group velocity, this quantity turns to zero at the cusp [see Fig. 7(b)]. Thus the mode corresponding to the cusp cannot be associated with a particular direction of propagation. It implies that this mode does not travel with respect to the laboratory frame of reference and, hence, it may be self-sustained without any reflections from the endwalls.

The cusp can be seen in Fig. 7(a) to correspond to the minimum of the marginal Marangoni number, which regarded as a function of k_r gives

$$\frac{\partial\ \mathrm{Ma}}{\partial k_r} = \frac{\partial\ \mathrm{Ma}}{\partial \omega_i}\frac{\partial \omega_i}{\partial k_r} = 0,$$

from which the imaginary part of the group velocity is seen to be zero at the given point. Since this point of zero group velocity is formed by merging of two oppositely traveling waves, it satisfies the Briggs pinching criterion [21] defining the threshold of the absolute instability. Note that a corresponding cusp map in the complex frequency plane was suggested in Ref. [22] for the detection of the absolute instability.

As seen in Fig. 6, the absolute transverse wave instability like the convective one exists only for sufficiently large Prandtl numbers ($\mathrm{Pr} > 1$). Note that disappearance of the convective instability below $\mathrm{Pr} = 0.18$ is related to the hydrodynamic stability of the corresponding basic flow [18]. The difference between both thresholds diminishes with the increase of Pr, so that they become hardly distinguishable. However, such a proximity of both these thresholds is not a general rule. As will be seen later, there may be a drastic difference between both thresholds when the buoyancy becomes significant.

B. Oblique waves

According to Smith and Davis [1], the convectively most unstable disturbance for thermocapillary driven flow is oblique rather than transverse. Analogically, the transverse waves are not granted to be the most unstable ones with respect to a self-sustained instability. For the following analysis it is important to note that the problem under consideration is spanwise mirror symmetric. Because the transverse waves remain invariant upon such reflections, the spanwise component of the group velocity must be zero, implying that these waves propagate strictly streamwise. But this is not so for oblique waves whose spanwise component of the group velocity may in general be nonzero. In the course of propagation, oblique waves can encounter and be reflected not only by the end walls, but also by the sidewalls. The mirror symmetry implies that for each oblique wave there is a spanwise mirror-reflected counterpart with the same streamwise, but an opposite spanwise direction of propagation. Thus a pair of mirror-symmetric oblique waves may be mutually coupled by reflections from the sidewalls. Further, if some oblique wave turns spatially amplified in the spanwise direction, the amplitude of such a wave can increase in course of multiple reflections from the sidewalls of a sufficiently wide system. Consequently, a neutrally stable global state requires at least a couple of mirror-symmetric oblique waves having spanwise invariant amplitude given by $\mathcal{I}[k_y] = 0$. However, such a pair of spanwise self-sustained waves may in general drift streamwise, and so leave the system without causing any self-sustained instability. The streamwise feedback necessary for the onset of a self-sustained instability requires an additional couple of mirror-symmetric oblique waves with a streamwise direction of propagation opposite to that of the first pair.

Let us concentrate further on the particular case where each pair of waves propagating in the same spanwise, but opposite streamwise directions, like the transverse waves considered in V A, merge together in a single oblique wave. The resulting globally neutral state is constituted by a single couple of mirror-symmetric waves propagating strictly spanwise in opposite directions with a spanwise-invariant amplitude. Comparing to the transverse waves, now there is one real quantity more involved, i.e., the spanwise component of the wave vector $k_{r,y} = \mathcal{R}[\mathbf{e}_y \cdot \mathbf{k}]$, which may formally be regarded as an additional control parameter like Ma. The problem to be solved is nearly the same as that of the absolute instability for the transverse waves, except that the corresponding threshold now is a function of $k_{r,y}$. The minimum of this threshold over $k_{r,y}$ gives the critical Marangoni number for the onset of the self-sustained instability which is analogous to the absolute one in the streamwise direction, but to the global one in the spanwise direction.

The critical Marangoni numbers corresponding to the thresholds of both convective and self-sustained instabilities for the basic flow driven purely by thermocapillarity ($\mathrm{Bo} = 0$) are plotted versus Prandtl number in Fig. 8(a). It is evident that the oblique disturbances are indeed more dan-

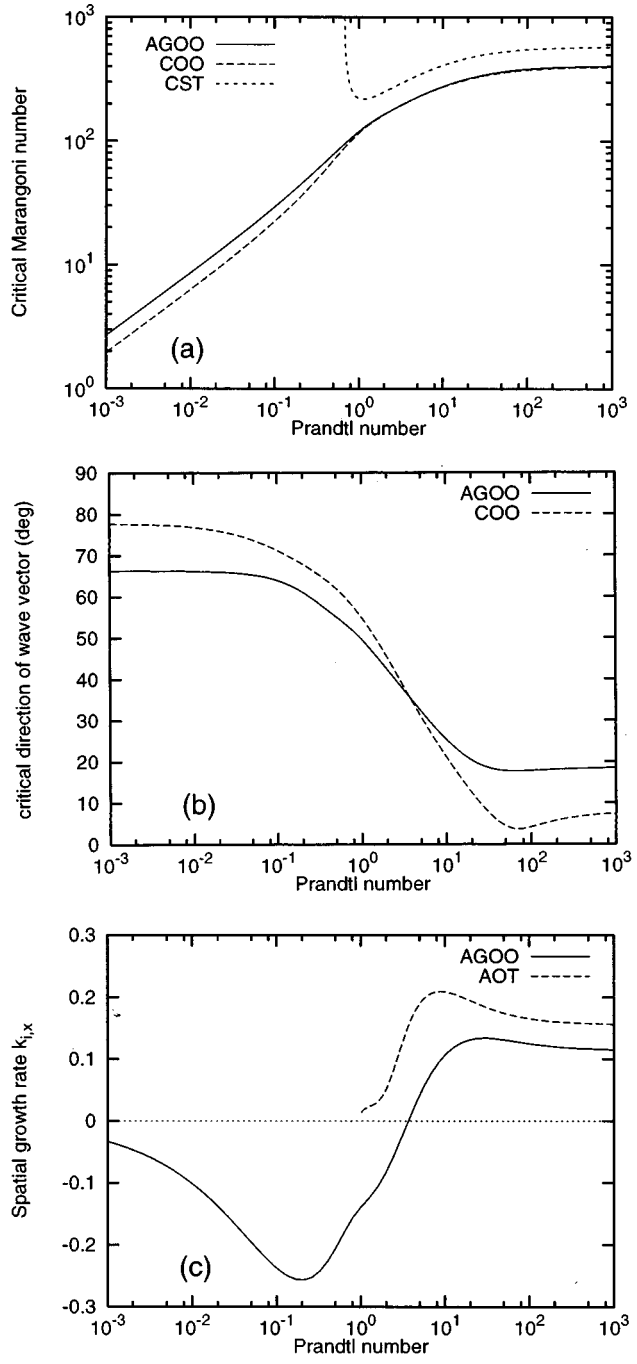

FIG. 8. Critical Marangoni numbers (a), directions of the wave vector (b), and the streamwise spatial growth rates ($k_{i,x}=\mathcal{I}[\mathbf{e}_x\cdot\mathbf{k}]$) (c) vs Prandtl number for various instability thresholds of thermocapillary driven basic flow (Bo$=0$). AGOO, COO, CST, AOT denote absolute global oblique oscillating, convective oblique oscillating, convective stationary transverse, and absolute oscillating transverse wave instabilities, respectively.

gerous with respect to a self-sustained instability than the transverse ones. Although the threshold of self-sustained instability is in principle higher than that of the convective instability, the difference between both is small, particularly for Pr>1. Nevertheless, there is a noticeable difference in the directions of the critical wave vectors for both types of instability [see Fig. 8(b)]. In contrast to the conventional stability theory, the given analysis predicts the amplitude of

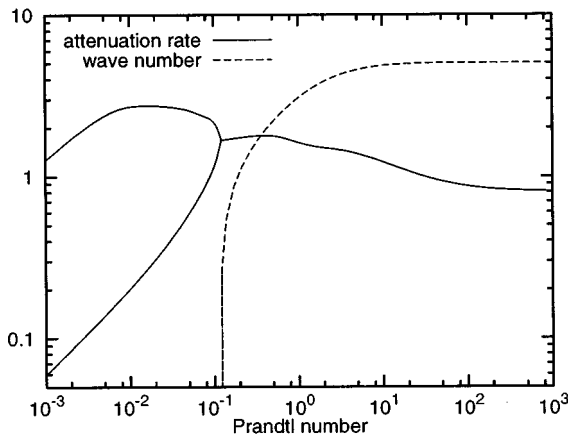

FIG. 9. Dimensionless spatial attenuation rate and wave number vs Prandtl number for the dominating upstream stationary wave induced by the hot end wall at the threshold of absolute-global instability of thermocapillary-driven basic flow (Bo$=0$).

the critical perturbation to be exponentially varying in the streamwise direction. The streamwise spatial growth rate $k_{i,x}=\mathcal{I}[k_x]$ versus Pr is plotted in Fig. 8(c). Note that for Pr>5, where $k_{i,x}>0$, the amplitude decreases in the positive direction of the x axis, which is downstream with the free surface velocity, whereas for Pr<5 it increases.

In addition, it may be seen in Fig. 8(a) that the threshold of the absolute-global instability, in contrast to the absolute one of transverse waves (see Fig. 6), is lower for all Pr than the threshold for stationary cells due to the hot end wall. This means that the self-sustained instability due to traveling oblique waves sets in before the stationary cells become spatially amplified and spread over the whole layer, provided the latter is extended enough. Since the extension of real layers is limited, the spatial attenuation rate of stationary waves is also of practical significance. The downstream attenuation rate and the corresponding wave number of the stationary perturbation occurring at the threshold of absolute-global instability are plotted in Fig. 9. It is evident that for Pr>0.12 this disturbance is spatially oscillating, and decays over a distance comparable to the depth of the layer, whereas for Pr<0.12 the decay becomes monotonic and occurs over a distance increasing with decrease of Pr. So, for Pr$\sim 10^{-2}$ the influence of the hot end wall can spread over tens of the layer depth.

VI. COMPARISON WITH EXPERIMENT

It turns out that with an increase of the buoyancy effect the threshold of the instability observed in the experiment [2] begins to differ strongly from that supplied by the conventional stability analysis [1,6]. The conventional theory predicts an oscillatory instability to be always the most dangerous one, whereas the experiment shows a stationary instability developing first for sufficiently large Bond numbers. The present approach in contrast to the conventional one proposes a physical mechanism of the stationary instability whose threshold is seen in Fig. 10 to be in good agreement with the corresponding experimental findings. Note that the experimentally detected threshold is slightly lower than the theoretical one, especially at larger Bond numbers.

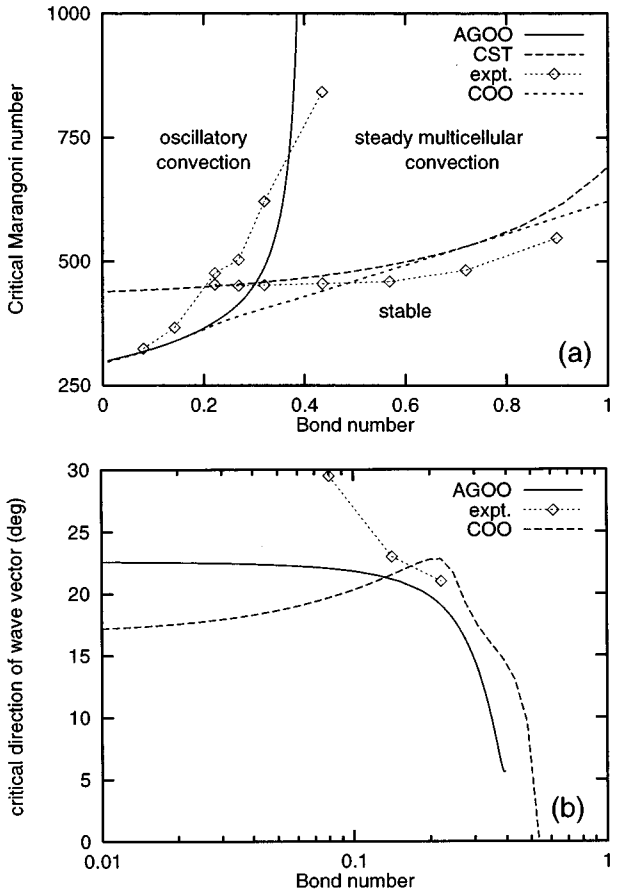

FIG. 10. Experimental and theoretical critical Marangoni numbers for the onset of both steady multicellular (CST) and oscillatory convection (AGOO) (a) and the corresponding angle between the critical wave vector and x axis (b) depending on the Bond number for 1-cS silicon oil ($\mathrm{Pr}=13.9$). The convective oscillating oblique wave instability (COO) results from the conventional theory.

This slight difference may be because of the continuous proceeding of the spatial attenuation rate to zero as the Marangoni number approaches the corresponding threshold. Thus a liquid layer of a limited extension might seem as covered by a steady wave pattern of apparently constant amplitude already before the attenuation rate becomes exactly zero.

In addition, the experimentally detected threshold of oscillatory instability, which for $\mathrm{Bo}\approx 0.2$ begins to differ strongly from that of the convective instability, is seen in Fig. 10 to be in good agreement with the threshold of the absolute-global instability introduced in this paper. However, note that for $\mathrm{Bo}>0.2$ the stationary wave developing from the hot end wall covers the whole layer before the oscillatory instability sets in. Thus the last occurs on a basic state being already disturbed by the first. This disturbance, which is neglected here, may be responsible for the remaining difference between theoretical and experimental thresholds noticeable in Fig. 10. Further development of the theory requires the analysis of nonlinear effects.

VII. SUMMARY AND CONCLUSIONS

This study dealt with the linear stability of thermocapillary-buoyancy-driven convection in a horizontal extended liquid layer subject to a longitudinal temperature gradient. The concepts of convective, absolute, and global instabilities are applied to calculate the thresholds of experimentally observed spatial and temporal oscillations of the flow. First, the conventional approach, based upon the concept of convective instability, is critically discussed. Second, the concept of the global instability for a spatially homogeneous system is presented in physically obvious terms by considering the virtual reflection of waves from distant confining boundaries. It is proven that the direction of propagation of the wave mode having the highest temporal growth rate for a given frequency and spatial growth rate is correctly determined in an active medium by the sign of the real part of the group velocity. The proposed criterion in contrast to the conventional one is local in the complex frequency plane and, therefore, it is more convenient for practical application.

We consider the effect of the boundaries on the spatially homogeneous basic state purely due to the thermocapillary effect. The principal idea is that distant lateral boundaries, besides reflecting waves, may be regarded also as a permanent stationary disturbance of the homogeneous basic state. The problem is to determine how far this perturbation penetrates into the homogeneous basic state. Within the framework of linear theory, the solution of the problem is given by the spatial attenuation rate (imaginary part of the wave number) of zero frequency mode. For large Reynolds numbers ($\mathrm{Re}\to\infty$) the attenuation length increases proportionally with Re, but within the purely hydrodynamic approximation ($\mathrm{Pr}=0$) it remains finite for any bounded Re. Coupling of temperature and hydrodynamic perturbations, which takes place at nonzero Pr, results in a negative downstream asymptotic attenuation when $\mathrm{Pr}>0.67$. This means that for $\mathrm{Pr}>0.67$ and sufficiently large Reynolds number the stationary wave induced by the upstream (hot) end wall may turn spatially amplified and spread over the whole layer regardless of its extent. Since the wave number of the stationary constant amplitude wave which first covers the whole layer is purely real, such a wave develops beyond the threshold of convective instability of the zero-frequency mode.

The analysis of self-sustained traveling waves is based on the concept of the global instability of spatially homogeneous systems. The mechanism of this instability is provided by virtual reflections of convectively unstable waves from distant lateral walls. The simplest neutrally stable self-sustained state is formed by the transverse waves coupled by reflections from the end walls, so that the spatial amplification rate of one wave compensates for the attenuation rate of the other. The most unstable transverse wave state is found to occur when the wave numbers of both waves belonging to the same branch merge together. This corresponds to the case of the absolute instability. The most dangerous self-sustained instability is caused by oblique rather than purely transverse disturbances. Such a self-sustained state comprises in general two couples of spanwise mirror-symmetric oblique waves. The most unstable state is formed when two waves propagating streamwise in the opposite, but spanwise in the same directions merge together. This results in a single oblique wave propagating strictly spanwise. The critical global mode comprises a couple of such mirror-symmetric oblique waves. This resembles the absolute instability streamwise but the global one spanwise.

When the basic state is purely due to thermocapillarity, the threshold of the global instability is only slightly higher than that of the convective instability. For $Pr > 1$, the effect of the buoyancy results in a drastic rise of the global instability threshold above the convective one. Moreover, under the effect of buoyancy the stationary perturbation due to the upstream end wall turns convectively unstable and spreads over the whole layer before the onset of oscillatory convection because of the global instability. The thresholds of both oscillatory and stationary wave instabilities calculated for a layer of 1-cS silicon oil are found to be in good agreement with the corresponding experimental data [2].

ACKNOWLEDGMENTS

We thank G. P. Neitzel for providing us experimental results. We are grateful to A. Gailitis for interesting and useful discussions. This work was supported by the German Space Agency (DARA).

[1] M. K. Smith and S. H. Davis, J. Fluid Mech. **132**, 119 (1983).
[2] R. J. Riley and G. P. Neitzel, Bull. Am. Phys. Soc. **39**, 1978 (1994); **40**, 2037 (1995); J. Fluid Mech. (to be published); and (private communication).
[3] D. Villers and J. K. Platten, J. Fluid Mech. **234**, 487 (1992).
[4] A. B. Ezersky, A. Garcimartín, H. L. Mancini, and C. Peréz-García, Phys. Rev. E **48**, 4414 (1993).
[5] F. Daviaud and J. M. Vince, Phys. Rev. E **48**, 4432 (1993).
[6] P. M. Parmentier, V. C. Regnier, and G. Lebon, Int. J. Heat Mass Transf. **36**, 2417 (1993).
[7] R. J. Deissler, Physica D **25**, 233; Phys. Fluids **30**, 2303 (1987); J. Stat. Phys. **54**, 1459 (1989).
[8] P. Huerre and P. A. Monkewitz, Annu. Rev. Fluid Mech. **22**, 473 (1990).
[9] L. Landau and E. M. Lifshitz, *Fluid Mechanics* (Pergamon, London, 1959).
[10] E. M. Lifshitz and L. P. Pitaevskii, *Physical Kinetics* (Pergamon, London 1981).
[11] A. G. Kulikovskii, Prikl. Mat. Mekh. **30**, 148 (1966) [J. Appl. Math. Mech. **30**, 180 (1966)].
[12] P. A. Sturrock, Phys. Rev. **112**, 1488 (1958).
[13] A. Bers, in *Basic Plasma Physics I*, edited by A. A. Galeev and R. N. Sudan (North-Holland, New York, 1983).
[14] R. Q. Twiss, Phys. Rev. **88**, 1392 (1952).
[15] A. Gailitis (private communication).
[16] J. Priede and G. Gerbeth, Phys. Fluids **9**, 1621 (1997).
[17] D. R. Gardner, S. A. Trogdon, and R. W. Douglass, J. Comput. Phys. **80**, 137 (1989).
[18] J. Priede and G. Gerbeth, J. Fluid Mech. **347**, 141 (1997).
[19] J. A. T. Bye, J. Fluid Mech. **26**, 577 (1966).
[20] P. Laure, B. Roux, and H. Ben Hadid, Phys. Fluids A **2**, 516 (1990).
[21] J. R. Briggs, *Electron-Stream Interaction with Plasmas* (MIT Press, Cambridge, MA, 1964).
[22] K. Kupfer, A. Bers, and A. K. Ram, Phys. Fluids **30**, 3075 (1987).